Optimizing the Connection Time for LEO Satellite Based on Dynamic Sensor Field

Tuyen Phong Truong[1(✉)], Hoang Van Tran[1], Hiep Xuan Huynh[2], and Bernard Pottier[1]

[1] Université de Bretagne Occidentale, Brest, France
{phong-tuyen.truong,pottier}@univ-brest.fr, tvhoang@ctu.edu.vn
[2] Can Tho University, Can Tho, Vietnam
hxhiep@ctu.edu.vn

Abstract. In this paper, we propose a new approach to optimize the connection time for Low Earth Orbit (LEO) satellite based on dynamic sensor field. A dynamic sensor field is a long range sensor network that is able to redefine the gateway for extension communication time with LEO satellite to adapt with the shift of the satellite's ground track at each revolution. The model for optimization comprises the parameters of both ground and space segment. The experimental results are performed on two sensor field deployments which aim at optimizing the connection time for successful communication.

Keywords: Connection time · LEO satellite · Satellite communications · Satellite orbit · Sensor field

1 Introduction

Wireless Sensor Network (WSN) [2] is known as a network of sensors cooperatively operating in order to surveillance or collect the environmental parameters. In addition, a sensor field is included a number of devices that can interact with one another and also to the environment. Most of existing wireless technique aims at short range application in aspect of smart cities such as parking allocation, home services, and so on [1,4]. Although the short transmission range can be compensated by applying a mesh topology, it would be economically infeasible to deploy in large geographic areas or behind obstacles (mountains, oceans, ...). To overcome these disadvantages, a long range wireless sensor network is proposed as a field of nodes (sensors or/and actuators) networking wirelessly in a far distance.

LEO satellites are classified into Sun synchronized [19]. Due to the Earth's rotation, the orbit of LEO satellite is shifted in westward direction around the polar axis at each revolution, as shown in Fig. 1 [1]. It leads to the meeting points of a gateway on the Earth's surface and the LEO satellite will be changed over time. Moreover, gateways can only communicate with LEO satellites when the satellites in their visibility region, generally in a short time approximately

P.C. Vinh and V. Alagar (Eds.): ICCASA 2015, LNICST 165, pp. 380–394, 2016.
DOI: 10.1007/978-3-319-29236-6_36

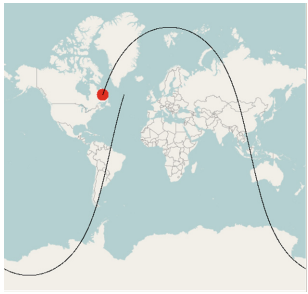

Fig. 1. LEO satellite's trajectory westward shifts because of the Earth's rotation [1].

5–10 min [5]. With a static sensor field, it can be occasionally unsuccessful in communication with the LEO satellite because the meeting time do not enough for data exchange.

A dynamic sensor field, which has the ability to redetermine its gateway to adapt with the shifts of LEO satellite's paths, is suitable to improve the connection time. To optimize the connection time, it is necessary to choose proper gateways for the longest length of connection time. Therefore, the connections between a LEO satellite and a dynamic sensor field is presented by graph-based model because it is convenient to observe and apply the optimization algorithms. In this paper, we propose a new approach based on dynamic sensor field to optimize connection time for LEO satellites.

The remainder of this paper is organized as follows. In Sect. 2, we overview related works. Section 3 presents a dynamic sensor field model. How to optimize the connection time between a sensor field and a LEO satellite based on dynamic sensor field is presented in Sect. 4. Section 5 gives two experiments of optimizing the connection time before a conclusion is drawn.

2 Related Work

In the last decade, researches on communication services provided by LEO satellites have focused on several main directions as follows.

Almost studies in LEO satellite design aim at optimizing the design the mechanics, interconnections, electric circuits, power supply to increase the lifetime of satellites [4,18].

Besides, many papers present about orbit design work, for example [5,20,21]. These researches focus on design satellites' trajectory, handover traffic and constellation for better operations in missions. Some of surveys also address the related issues of cooperating and optimizing the positions of ground stations in order to improve the durations of communications, as can be seen in [3,13].

On another approach, many surveys show the research topics in the optimization of communications that attracts so many researchers. They work on protocols, radio frequencies, onboard transceivers and antenna designs to enhance

the quality of communication services with a low power consumption which were introduced in so many technical papers such as [6,16,17].

The LEO satellite communication can be used in mobile satellite communications, surveillance the Earth surface, geological surveys, so on [4]. However, the direct radio links between sensor fields and LEO satellites are not considered in literature. In recent years, it emerges as an attractive topic because of the current innovation solutions such as LoRa Semtech and solutions from vendors QB50 [1,8].

3 Dynamic Sensor Field

3.1 Sensor Field

A sensor field (SF) [7] is presented by a graph G(V, E) with a set of vertices $V = \{v_1, v_2, ..., v_n\}$ and a set of edges $E = \{e_1, e_2, ..., e_m\}$ with $e_k = e(v_i, v_j)$, $k = 1..m$, $i = 1..n$, $j = 1..m$, $m = 2^n$. The weights of these edges are defined by $W = \{w_1, w_2, ..., w_m\}$ where the value of each w_k is given by function $f_1()$, $w_k = f_1()$ (Fig. 2).

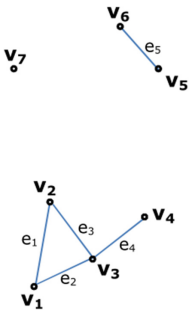

Fig. 2. A graph of a sensor field with 7 vertices (nodes) $V = \{v_1, v_2, v_3, v_4, v_5, v_6, v_7\}$ and 5 edges $E = \{e_1 = e(v_1, v_2), e_2 = e(v_1, v_3), e_3 = e(v_2, v_3), e_4 = e(v_3, v_4), e_5 = e(v_5, v_6)\}$.

Each node of SF has a maximum communication range that is indicated by a circle with radius r. In order to define the conditions to exist an edge, we introduce two following definitions:

Definition 1 (Established Edge). An edge is established if and only if the distance between a pair of vertices is less or equal to the minimum value of their radii, $d_(v_i, v_j) \leq \min(r_i, r_j)$.

Definition 2 (Not Established Edge). An edge is not established if the distance between a pair of vertices is greater than the minimum value of their radii, $d_(v_i, v_j) > \min(r_i, r_j)$.

As can be seen in Fig. 3, a pair of vertices (v_5, v_6) have the same maximum communication range that is indicated by two solid red circles with radius r.

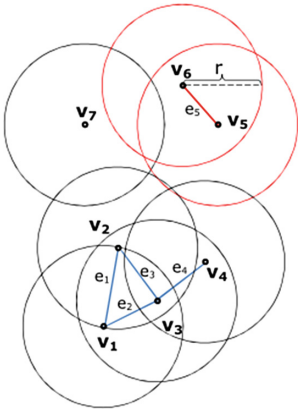

Fig. 3. The graph of a sensor field. The maximum communication range of nodes that is indicated by two solid red circles with radius

Because the distance between v_5 and v_6 is less than r, $d(v_5, v_6) < r$, based on *D*efinition 1 there exists an edge e_5 connecting them. Similarly, the others edges of this graph namely $e_1 = e(v_1, v_2), e_2 = e(v_1, v_3), e_3 = e(v_2, v_3), e_4 = e(v_3, v_4)$ could be established. There are $2^n - 5$ edges between a pair of vertices of this graph that are not existed due to adequacy of Definition 2. Note that vertex v_7 is isolated because all distance values between it and the other vertices are inadequate to the *D*efinition 1.

3.2 Extended Sensor Field

An extended sensor field (ESF) is used to describe a sensor field in the connection with a LEO satellite. When a LEO satellite connects with a sensor field, its sub-point on the ground (sub-satellite point) is considered as a center vertex, s, of the graph. Consequently, the graph consists of $n + 1$ vertices $P = \{V, s\} = \{v_1, v_2, ..., v_n, s\}$. In addition, the number edges of the graph are $m+n$ by adding

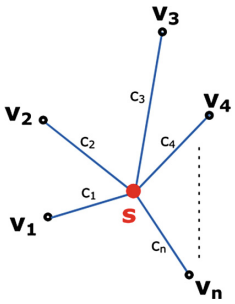

Fig. 4. A star graph of the connections between center vertex s (a sub-satellite point) and other vertices $\{v_1, v_2, ..., v_n\}$ (nodes of a sensor field).

n new edges $C = \{c_1, c_2, ..., c_n\}$ with $c_i = c(s, v_i)$, $i = 1..n$. The weights of the n new edges are defined by $Z = \{z_1, z_2, ..., z_n\}$ where the value of each z_i is given by function $f_2()$, $z_i = f_2()$. Hence, in this case the set of edges is $R = \{E, C\} = \{e_1, e_2, ..., e_m, c_1, c_2, ..., c_n\}$ and the set of corresponding weights is $Q = \{W, Z\} = \{\{w_k\}, \{z_i\}\}$ with $k = 1..m$, $i = 1..n$. As a result, the ESF is presented by a graph G(P,R).

Figure 4 illustrates a star graph of the connections between a center vertex s (a sub-satellite point on the Earth's surface) and a set of n vertices, $V = \{v_1, v_2, ..., v_n\}$ (nodes of a SF). It is noted that sub-satellite point, s, is where on the ground the straight line connecting the center of the Earth and the satellite meets the Earth's surface. If the satellite and any node can communicate with each other, there exists an edge between them. Thus, n direct connections between s and the set of vertices are indicated by a set of n edges $C = \{c_1, c_2, ..., c_n\}$.

3.3 Dynamic Sensor Field

To describe a dynamic sensor field (DSF) in connections with a LEO satellite, we propose two definitions as follows:

Definition 3 (Connection Vector). Connection vector is a vector which stores vertices in set $V = \{v_1, v_2, ..., v_n\}$ connecting with center vertex s in chronological order.

Definition 4 (Time Vector). Time vector is a vector which stores time of the corresponding connections in *Vector connection*.

In a dynamic sensor field, only one vertex (node) in set $V = \{v_1, v_2, ..., v_n\}$ is chosen to connect with the center vertex (sub-satellite point), s, at a time. Generally, different nodes could be chosen based on the set of weights at different times. The name of chosen node is stored in *Connection vector* and the corresponding time is stored in *Time vector*.

Connection number	1	2	3	...
Connection vector	v_1	v_4	v_2	...
Time vector	t_1	t_2	t_3	...

Fig. 5. An example of satellite connection data with three rows: *Connection number*, *Connection vector* and *Time vector*.

Figure 5 shows that in *connection 1*, center vertex s establishes the connection with v_1 at time t_1. In a similar way, in *connection 2* at time t_2 and *connection 3* at time t_3, v_4 and v_2 are chosen to connect with s respectively.

Three graphs of the dynamic sensor field in three different connections with the center vertex, s, at different times t_1, t_2 and t_3 are shown in Fig. 6. At time t_1 (see Fig. 6(a)), vertex v_1 is chosen and edge c_1 is established. Similarly, in Fig. 6(b) and (c) vertex v_4, v_2 are chosen that leads to c_4, c_2 are established at time t_2 and t_3 respectively.

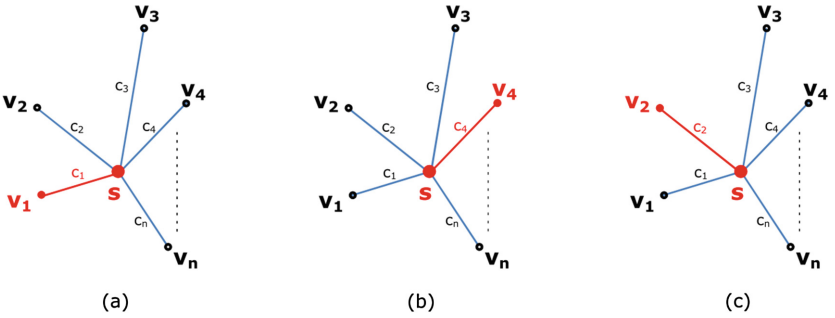

Fig. 6. The graph of a dynamic sensor field with three different connections (solid red lines) at time t_1, t_2 and t_3.

4 Connection Optimization

4.1 Compute the Connection Time

In this section, we describe the way to calculate connection time, f_2, between a LEO satellite and a gateway of DSF, v_i [19,22]. Similarly, the calculation could be applied for all other nodes. Note that every node of the sensor field is assumed as a gateway for the connection with the satellite in calculating the values of connection time.

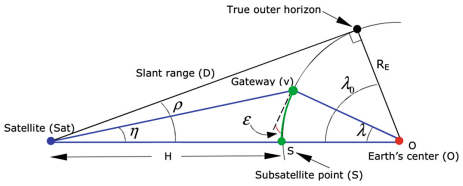

Fig. 7. Gateway of sensor field geometry [19].

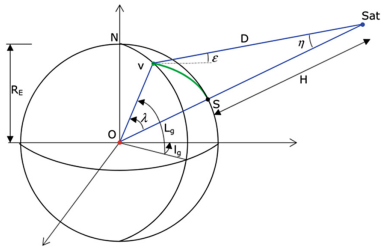

Fig. 8. Geometrical relation between sub-satellite point (S) in coordinate frame [19].

First, it is necessary to define the angles and related distances between satellite, a gateway on the ground and the Earth's center. The parameters are indicated on Figs. 7 and 8. For angular radius of the spherical Earth, ρ_i, can be found from relation

$$\sin(\rho_i) = \frac{R_E}{R_E + H} \tag{1}$$

where $R_E = 6378.14$ km is the Earth's radius and H is the altitude of the satellite above the Earth's surface.

In this work, we assume that connection duration is the amount of time when a gateway is still under the access area of LEO satellite with $\varepsilon_i \geq 5\ deg$, therefore $\varepsilon_{i_{min}} = 5\ deg$. With the value of $\varepsilon_{i_{min}}$, the values of *maximum Earth central angle*, $\lambda_{i_{max}}$, *maximum nadir angle*, $\eta_{i_{max}}$, and *maximum slant range*, $D_{i_{max}}$, can be computed by the following equations:

$$\sin(\eta_{i_{max}}) = \sin(\rho_i)\cos(\varepsilon_{i_{min}}) \tag{2}$$

$$\lambda_{i_{max}} = 90\ deg - \varepsilon_{i_{min}} - \eta_{i_{max}} \tag{3}$$

$$D_{i_{max}} = R_E \frac{\sin(\lambda_{i_{min}})}{\sin(\eta_{i_{max}})} \tag{4}$$

The maximum Earth central angle, $\lambda_{i_{max}}$ is defined as the radius of the access area. The double of $\lambda_{i_{max}}$ value is the ground track's swath width. From Fig. 9, the maximum value of the instantaneous access area, $IAA_{i_{max}}$, of a gateway on the Earth's surface will be defined by

$$IAA_{i_{max}} = 2\pi R_E^2(1 - \cos(\lambda_{i_{max}})) \tag{5}$$

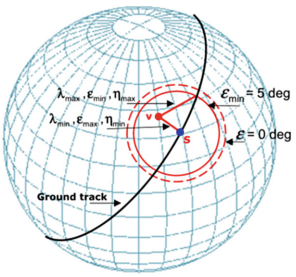

Fig. 9. Determination of the coverage for LEO satellite [19].

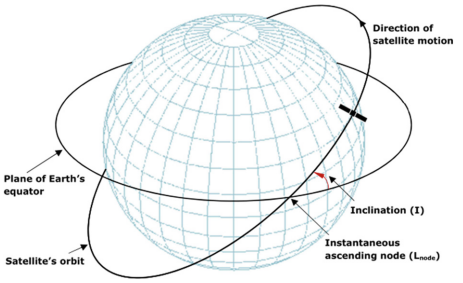

Fig. 10. A LEO satellite on its orbit [19].

As can be seen on Fig. 10, the orbit of a LEO satellite is specified by two main parameters namely the inclination angle, I, and longitude, L_{node}, of the instantaneous ascending node. In Earth geometry, these parameters often expressed in terms of the pole of the orbit plane with coordinates as

$$lat_{pole} = 90\ deg - I \tag{6}$$

$$long_{pole} = L_{node} - 90\ deg \tag{7}$$

From the geometry of Fig. 8, knowing the latitude and longitude of both the orbit pole and the gateway the value $\lambda_{i_{min}}$ can be found from

$$\sin(\lambda_{i_{min}}) = \sin(lat_{pole})\sin(lat_{g_i}) + \cos(lat_{pole})\cos(lat_{g_i})\cos(\Delta long_i) \tag{8}$$

where $\Delta long_i$ is the longitude difference between the gateway and the orbit pole. Consider the satellite in a circular orbit, the *orbit period* in minutes, P, is related to altitude, H, in kilometers by

$$P = 1.658669 \times 10^{-4} \times (6,378.14 + H)^{3/2} \tag{9}$$

Finally, the *connection time*, f_{2_i}, is given by

$$f_{2_i} = (\frac{P}{180\ deg}) \arccos(\frac{\cos(\lambda_{i_{max}})}{\cos(\lambda_{i_{min}})}) \tag{10}$$

4.2 Define the Operation Modes of DSF

In order to describe the behaviors of a dynamic sensor field, we propose two definitions as follows:

Definition 5 (Passive Mode). Passive mode of a dynamic sensor field is established when a dynamic sensor field automatically collects and prepares the environmental data to sent before visiting a LEO satellite. Each time the satellite is perceived, the gateway of sensor field will establish the connection and then send the data. All processes of a dynamic sensor field are programmed and repeated systematically.

Definition 6 (Active Mode). Active mode of a dynamic sensor field is established when a dynamic sensor field has the ability to response satellite's commands before the end of a contact. In this mode, a LEO satellite visits a dynamic sensor field and establishes a connection with a gateway. The satellite then sends a command to gateway for control purposes and/or collecting environmental data from DSF. After a certain period of time, it expects to receive the feedback data also via a gateway. Hence, there is a pair of gateways: *Input gateway* for receiving satellite's command at the starting time and *Output gateway* for sending data to satellite before the satellite leaving.

4.3 Constraint

The altitude of a LEO satellite must be in range from 275 km to 1400 km due to atmosphere drag and Van Allen radiation effects [3,19]. Besides, the experimental results were announced by High Altitude Society in United Kingdom that LoRa SemTech transceivers can communicate in distance up to 600 km in environment without any obstacle and 20–40 km in urban area [8]. Based on these factors, maximum communication range for all nodes in long range sensor fields is 40 km in this work. LEO's satellites are chosen in our experiments must have the orbit altitude less than 600 km. Furthermore, the satellite's relative speed over a fixed point on the Earth's surface must be around 7.5–8.0 km/sec [19]. The speed of the satellite is calculated by

$$v = \sqrt{\frac{Gm_E}{R_E + H}} \tag{11}$$

Equation 11 shows that the speed of the satellite in orbit is in inverse proportion of its altitude [19]. Where G is universal gravitational constant ($G = 6.67 \times 10^{-11}$ $\mathrm{Nm}^2/\mathrm{kg}^2$) and m_E is the mass of the Earth ($m_E = 5.98 \times 10^{24}$ kg). With orbit altitude of satellite in range 300–600 km, the speed of satellite on orbit must be in range 7.56–7.73 km/sec.

4.4 Optimization Method

In order to present the method of optimization for connection time, we introduce two following definitions:

Definition 7 (Sensorset). A sensorset is created whenever one or more nodes appear and/or disappear in a subset of nodes.

Let a DSF with n nodes, $V = \{v_i\}$, $i = 1..n$, and an extended node, s, which is the sub-satellite point of a LEO satellite. The problem is how to optimize the connection time between the DSF with a satellite. A sensorset $A_k = \{v_j\}$, $j = 1..m$ with $m \leq n$, is several nodes that the satellite can connect at a time. A_k is a subset of V so that the union of all subsets A_k in the period of time, $T = t_k$, $k = 1..p$ is set V, $V = A_1 \cup A_2 .. \cup A_p$. It is necessary to find out a set of proper nodes that provides the longest length of time for the connection. This leads to two following sub-problems:

Problem 1: Consider a sensorset, which node provides the longest connection duration time.

The connection times of all nodes are calculated and then sorted in a descending list. To obtain maximum connection time, the node corresponding to the value at the top of this list is selected to connect with the satellite.

The algorithm for selecting the gateways of the DSF is briefly presented as follows:

```
//Calculate connection durations
for i = 1 to n
    f2_i = Time4Con(Nodei.Position, SubSat.Position);
//Find the maximum value of connection durations
MaxVal = max{f2};
//Node, which has the maximum value of connection durations, will
become a gateway
if (f2_i = MaxVal) then
    UpdateConnectionData(i,Node_i,t);
```

Problem 2: Consider all nodes of a DSF, which set of nodes provide total of connection times which is the longest.

To select a proper set of nodes, the *association analysis algorithm* [23] is applied. If a DSF V has n nodes, there are $2^n - 1$ connection items, $G = \{g_l\}$, l=1..$(2^n - 1)$. The DSF is represented in a binary format, where each row corresponds to a connection item and each column corresponds to a node. A node value is one if the node appears in a connection item and zero otherwise. Weight of a connection item determines how often a connection item is applicable to a set of connection items. The weight of a connection item, $g_i \in G$, can be defined as follows:

$$w(g_i) = \mid \{g_l \mid g_i \subseteq g_l, g_l \in G\} \mid \tag{12}$$

where the symbol $\mid . \mid$ denotes the number of elements in a set.

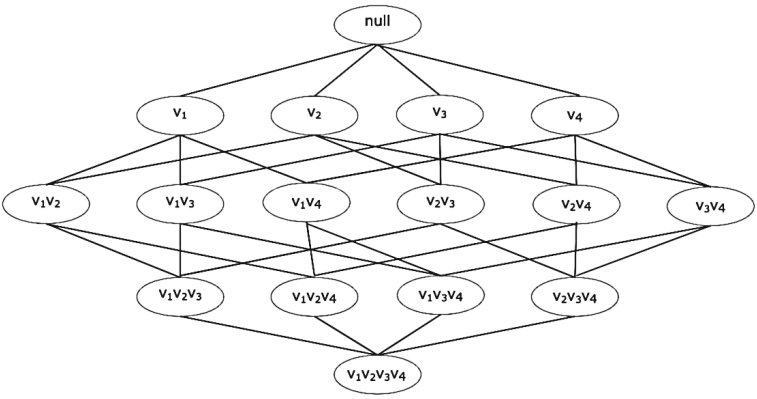

Fig. 11. A sensors lattice for a DSF $V = \{v_1, v_2, v_3, v_4\}$.

A lattice structure is used to enumerate the list of all possible connection items. In Fig. 11, a connection item lattice for a DSF $V = \{v_1, v_2, v_3, v_4\}$ is depicted. Connection item corresponding to the highest weight is chosen aim at achieving the longest length of connection time.

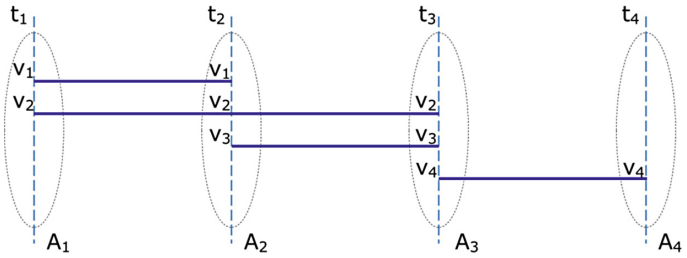

Fig. 12. The connections between a 4-node DSF with a LEO satellite.

For example, in Fig. 12 a DSF with 4 nodes, $V = \{v_1, v_2, v_3, v_4\}$. There are 4 sensorsets $A_1 = \{v_1, v_2\}$, $A_2 = \{v_1, v_2, v_3\}$, $A_3 = \{v_2, v_3, v_4\}$ and $A_4 = \{v_4\}$.

Connection items	Weights
(v_1, v_2, v_4)	1
(v_1, v_3, v_4)	1
(v_2, v_4)	3
(v_2, v_3, v_4)	1

Fig. 13. The weights of connection items in a DSF with 4 nodes.

The weights of connection items are presented in Fig. 13. Because the weight of connection item (v_2, v_4) is highest, this connection is chosen.

5 Experiment

5.1 Data Used

For experiments, there are two abstract structure of the long-range sensor fields for fire forest surveillance were generated by using NetGen [9]. Figure 14 shows the first dynamic sensor field consists of 50 sensor nodes (DSF50) that is stretched from South Central Coastal to Southeast and extended up to Mekong River Delta in Vietnam. The second dynamic sensor field contains 110 nodes (DSF110) that was deployed along Vietnam's border.

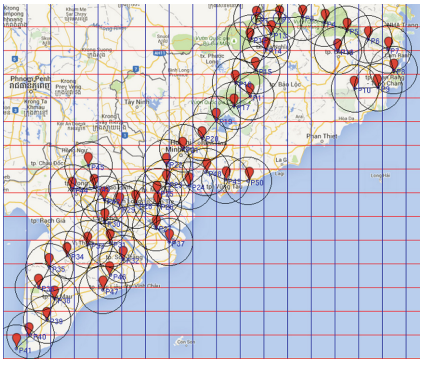

Fig. 14. A dynamic sensor field with 50 nodes (DSF50) was deployed by using NetGen.

According to the constraints about the satellite's orbit altitude as discussed in Sect. 4.3, BEESAT-3 [12] was chosen in this experiment. Thirty data orbits of BEESAT-3 were used as input data of optimization process (see Fig. 15). The data are stored in plain text (.txt files) that are used as input data. Figure 16 presents the structure of a orbit data (orbit 12794) after reforming.

12794	12795	12801	12802	12809	12810	12816	12817	12824	12825
12831	12832	12839	12840	12846	12847	12854	12855	12861	12862
12869	12870	12876	12877	12884	12885	12891	12899	12900	12906

Fig. 15. Thirty orbits of BEESAT-3 from 17 to 25 August 2015.

Time	Lat	Lon
17/08/2015 15:58:24	-9.81	117.00
17/08/2015 15:58:34	-9.24	117.23
...	...	...

Fig. 16. The orbit 12794 of BEESAT-3 after reforming.

5.2 DYNSEN Tool

We have developed the DYNSEN tool by Octave [14], that enables to optimize the connection time between a dynamic sensor field with a LEO satellite. GPredict [10] is used to provide the information about satellite path. Besides, NetGen tool [9] is utilized to generate the abstract network of two dynamic sensor fields from geographic data provided by Google maps service. The obtained result is nodes of the DSFs which should be configured as gateways for the best connection duration times.

5.3 Scenario 1: The Dynamic Sensor Field in Passive Mode

Thirty sensorsets are created with each satellite's orbit, during the period of time the BEESAT-3 visits the DSF50. With each sensorset, a subset of connections is established. The weights of each connection in subset are then computed. A set of connection items is created by combining these subsets. The best connection is chosen based on the weights of connection items. For instance, with orbit 12974 and 12795 node v_{08} and v_{44} are chosen corresponding to the connection time 6.5691 and 9.9812 min, respectively.

Orbit	Static Sensor Field		Dynamic Sensor Field	
	Gateway (lat, long)	Connection time (minutes)	Gateway (lat, long)	Connection time (minutes)
12794	**V30** (10.04, 105.74)	4.5182	**V08** (11.75, 109.10)	6.5691
12795	**V30** (10.04, 105.74)	9.9145	**V44** (10.40, 105.37)	9.9812

Fig. 17. The connection times of DSF50 in two BEESAT-3's orbits (12794, 12795) on August 17, 2015.

The gateways of DSF50 in two BEESAT-3's orbits (12794 and 12795) on August 17, 2015 are shown in Fig. 17. From the experimental results with the thirty different orbits of BEESAT-3, the dynamic gateway gives the longer length of time for connection than the static one.

The chart in Fig. 18 presents the average connection duration of the DSF50 in thirty orbits of BEESAT-3 and the corresponding the value of DSF110. It is obvious that in case of applying a dynamic gateway, the connection times are 8.16 and 8.41 min for DSF50, DSF110 respectively that are better than the values with a static gateway, 7.04 min. Consequently, the increment in connection duration is around 65–80 s which is equivalent to an increase of 15–20 %.

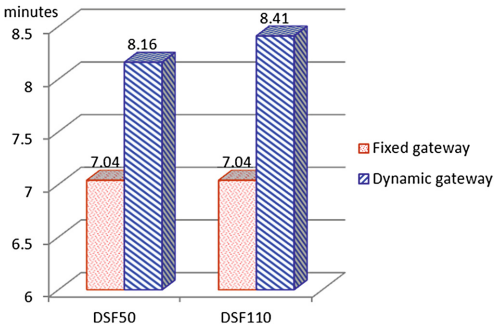

Fig. 18. The average of connection times of DSF50 and DSF110 over thirty different orbits of BEESAT-3.

5.4 Scenario 2: The Dynamic Sensor Field in Active Mode

In this scenario, the dynamic sensor field with 110 nodes is used in our experiments. We also use the information about ground track of two BEESAT-3's orbits (12794 and 12795) on August 17, 2015 as input data. The similar process as described in scenarios 1 is utilized, but in this case a pair of nodes must be chosen as *Input gateway* and *Output gateway* for the best connection time with each satellite's orbit.

Orbit	Input gateway (lat, long)	Output gateway (lat, long)
12794	V81 (11.70, 109.12)	V13 (20.31, 105.59)
12795	V109 (10.37, 104.80)	V03 (22.08, 104.06)

Fig. 19. Two pairs of *(Input gateway, Output gateway)* are chosen corresponding to two BEESAT-3's orbits (12794 and 12795) in August 17, 2015.

Figure 19 shows pairs of *(Input gateway, Output gateway)* for two BEESAT-3's orbits. With orbit 12794, v_{81} was selected as *Input gateway* and v_{13} was selected as *Output gateway*. However, with orbit 12795 (v_{109}, v_{03}) was a chosen as pair of *(Input gateway, Output gateway)*.

6 Conclusion

Based on the dynamic structure of a sensor field, we have described a new approach in order to optimize the connection time for LEO satellites. The distances between the sub-satellite point and each node of the sensor field is utilised for determination a pair of gateways to adapt with different satellite path. The experimental results were obtained by performing DYNSEN in two

different scenarios in which the dynamic sensor field was optimized to adapt with the shifts of satellite paths. With dynamic sensor field approach, the amount of time for communication could be improved in long-range sensor field applications using satellite connections to monitor, control and collect environmental data.

Acknowledgment. The author gratefully acknowledges the MOET-VIED (Ministry of Education and Training - Vietnam International Education Development) of the Vietnam Government for awarding a scholarship to the first author of this research.

References

1. Lucas, P.-Y., Van Long, N.H., Truong, T.P., Pottier, B.: Wire-less sensor networks and satellite simulation. In: 7th EAI International Conference onWireless and Satellite Systems (WiSATS 2015), Bradford, United Kingdom (2015)
2. Àlvarez, C., Duch, A., Gabarro, J., Serna, M.: Sensor field: a computational model. In: Dolev, S. (ed.) ALGOSENSORS 2009. LNCS, vol. 5804, pp. 3–14. Springer, Heidelberg (2009)
3. Cakaj, S., Fischer, M., Scholtz, A.L.: Practical horizon plane for low earth orbiting (LEO) satellite ground stations. In: TELE-INFO 2009 Proceedings of the 8th WSEAS International Conference on Telecommunications and Informatics, pp. 62–67. ACM Digital Library (2009)
4. Celandroni, N., et al.: A survey of architectures and scenarios in satellite-based wireless sensor networks: system design aspects. Int. J. Satell. Commun. Network. **31**(1), 1–38 (2013). Wiley
5. Cakaj, S., Kamo, B., Lala, A., Rakipi, A.: The coverage analysis for low earth orbiting satellites at low elevation. Int. J. Adv. Comput. Sci. Appl.(ijacsa), **5**(6) (2014)
6. Cakaj, Sh., Keim, W., Malaric, K.: Communication duration with low earth orbiting satellites. In: Proceedings of IEEE, IASTED, 4th International Conference on Antennas, Radar and Wave Propagation, Montreal, pp. 85–88 (2007)
7. Bayat, D., Habibi, D., Ahmad, I.: Development of a wireless sensor node for environmental monitoring. In: The Sixth International Conference on Sensor Technologies and Applications (SENSORCOMM), pp. 1–5. International Academy, Research, and Industry Association (IARIA) (2012)
8. UK High Altitude Society. http://www.instructables.com/id/Introducing-LoRa-/step19/LoRa-receiver-links/
9. Pottier, B., Lucas, P.-Y.: Dynamic networks NetGen: objectives, installation, use, and programming. Technical report, Universit de Bretagne Occidentale, France (2014)
10. Alexandru Csete, GPredict project. http://gpredict.oz9aec.net/
11. Google Maps services, the map of Vietnam. https://www.google.fr/maps/place/Vietnam/@15.9030623,105.8066791,6z/data=!3m1!4b1!4m2!3m1!1s0x31157a4d736a1e5f:0xb03bb0c9e2fe62be
12. Berlin Experimental and Educational Satellite-2 and -3. https://directory.eoportal.org/web/eoportal/satellite-missions/b/beesat-2-3
13. Cakaj, S.: Elevation variation with low earth orbiting search and rescue satellites for the station implemented in kosovo. Univers. J. Commun. Netw. **1**, 32–37 (2013). Horizon Research Publishing

14. Eaton, J.W.: GNU Octave 4.0.0. (2015). https://www.gnu.org/software/octave/
15. Dosiere, F., Zein, T., Maral, G., Boutes, J.P.: A model for the handover traffic in low earth-orbiting (LEO) satellite networks for personal communications. Int. J. Satell. Commun. pp. 574–578 (1993)
16. Fernandez Del Rio, J.E., Nubla, A., Bustamante, L., Van't Klooster, K: SOPERA: a new antenna concept for low Earth orbit satellites. In: Antennas and Propagation Society International Symposium, pp. 688–691. IEEE Press (1999)
17. Sreeja, T.K., Arun, A., Jaya Kumari, J.: An: S-Band Micro-strip Patch Array Antenna for nano-satellite applications. In: International Conference on Green Technologies (ICGT), pp. 325–328 (2012)
18. Abdi, B., Alimardani, A., Ghasemi, R., Mirtalaei, S.M.M.: Energy storage selection for LEO satellites. Int. J. Mach. Learn. Comput. **3**(3), 287–290 (2013)
19. Larson, W.J., Wertz, J.R.: Chapter 5: Space Mission Geometry. Space Mission Analysis and Design, 3rd edn, pp. 95–230. Microcosm Press, El Segundo (2003)
20. Muri, P., McNair, J.: A survey of communication sub-systems for intersatellite linked systems and CubeSat missions. J. Commun. **7**(4), 290–308 (2012)
21. Chowdhury, P.K., Atiquzzaman, M., Ivancic, W.: Handover Schemes in Satellite Networks: State-of-the-Art and Future Research Directions. Communications Surveys & Tutorials, **8**(4). IEEE express (2006) Signal Processing and Communications Perspectives, pp. 277–309. John Wiley & Sons Ltd (2207)
22. Capderou, M.: Chapter 8- Ground track of a statellite. Handbook of satellite orbits from Kepler to GPS, pp. 301–338. Springer International Publishing Switzerland (2014)
23. Tan, P.-N., Steinbach, M., Kumar, V.: Chapter 6 Association Analysis: Basic Concepts and Algorithms. Introduction to Data Mining, pp. 327–413. Addison-Wesley Longman Publishing Co., Inc., Boston (2005)